Simulated Structure Factors

Benjamin J. Coscia

July 10, 2018

1 Calculation of the structure factor

The structure factor, S($\mathbf{q}$), relates the observed intensity per atom to that observed by a single scattering unit. Incident plane waves falling on a material have a wave vector, K_i, whose length is $\frac{2\pi}{\lambda}$, where λ is the wavelength. The diffracted wave vector, K_f, has the same length as K_i if the diffraction process is elastic. We will assume elasticity going forward. The scattering vector, $\mathbf{q}$, is defined as $K_f - K_i$. Since K_f and K_i are the same length, the scattering vector must lie on the surface of a sphere of radius $\frac{2\pi}{\lambda}$. This sphere is called the Ewald Sphere and diffraction will only occur for reciprocal lattice points that lie on its surface.

The amplitude and phase of the scattered waves is the vector sum of all scattered waves from all atoms:

$$\Psi_s(\mathbf{q}) = \sum_{j=1}^{N} f_j e^{-i\mathbf{q}\cdot\mathbf{R_j}} \tag{1}$$

where f_j is the atomic form factor of atom j and $\mathbf{R_j}$ is the position of the atom in real space. Note that Equation 1 is the definition of the discrete fourier transform.

The scattered intensity is obtained by multiplying Equation 1by its complex conjugate:

$$I(\mathbf{q}) = \Psi_s(\mathbf{q}) \cdot \overline{\Psi_s}(\mathbf{q}) = \sum_{j=1}^{N} f_j e^{-i\mathbf{q}\cdot\mathbf{R_j}} \times \sum_{k=1}^{N} f_k e^{-i\mathbf{q}\cdot\mathbf{R_k}} = \sum_{j=1}^{N}\sum_{j=k}^{N} f_j f_k e^{-i\mathbf{q}\cdot(\mathbf{R_j}-\mathbf{R_k})} \tag{2}$$

Computationally, one should calculate the fourier transform of the atomic coordinates with a fast fourier transform, calculate its complex conjugate and multiply them together. The structure factor is typically normalized as $1/\sum_{j=1}^{N} {f_j}^2$ so that it is independent of system size, and the general equation for the structure factor becomes:

$$S(\mathbf{q}) = \frac{1}{\sum_{j=1}^{N} {f_j}^2} \sum_{j=1}^{N}\sum_{j=k}^{N} f_j f_k e^{-i\mathbf{q}\cdot(\mathbf{R_j}-\mathbf{R_k})} \tag{3}$$

If all atoms are identical, Equation 2 simplifies to:

$$S(\mathbf{q}) = \frac{1}{N} \sum_{j=1}^{N}\sum_{j=k}^{N} e^{-i\mathbf{q}\cdot(\mathbf{R_j}-\mathbf{R_k})} \tag{4}$$

The atomic form factor, f_j is more complicated than how it is represented in Equation 1 The atomic form factor is the scattering contribution from a single isolated atom. They are calculated as the fourier transform of the electron density, $\rho(\mathbf{r})$, which is typically calculated using quantum techniques. Since $\rho(\mathbf{r})$ is a spatially dependent function, f_j is actually a function of $\mathbf{q}$, $f(\mathbf{q})$. Values of $f(\mathbf{q})$ for each element are tabulated in the International Tables for Crystallography. For $\mathbf{q} = \mathbf{0}$, the atomic form factor is equal to the number of electrons possessed by the atom.

The resolution in each dimension of reciprocal space is determined by the size of the unit cell studied. In order to calculate the structure factor, the system's 3D coordinates must be discretized into regularly sampled points using a histogramming method. Applying equation 2 to the histogram will yield a grid with

Fourier bin sizes of $\frac{2\pi}{L_i}$ (i = (x,y,z)). The fourier transform of an array of values returns a same length array of frequencies. Increasing the number of bins in the histogram will not change the size of the Fourier space bins, rather it will increase the maximum accessible value of q.

2 Structure factor of hexagonally packed columns

Here, we explore, in depth, a simplified model of an inverted hexagonal phase lyotropic liquid crystal (H_{II} LLC). The simplified model is meant to enhance our understanding of the structure factor of a fully atomistic model of the same material. We are primarily interested in the diffraction patterns produced by the head groups so we model each monomer as a point placed at the center of mass of its head group. The hexagonal phase is made of straight pore columns. Each pore column is composed of columns of stacked monomers which surround the pore's hydrophilic core. Based on simulation, there are likely 5 monomer columns making up each pore, and the pore radius is ca. 1 nm. Experimental WAXS suggests that monomers stack 3.7 Åapart, and SAXS measurements have shown that pores are spaced ca. 4.1 nm apart. Here, unless otherwise noted we took the pore spacing to be 4.25 nm for no good reason. For consistency with simulation, we will look at 4 pores in a monoclinic unit cell with 5 monomer columns per pore, unless specified otherwise.

We are interested in the intensity and dimensions of the R-π reflection, which is a consequence of monomers stacked on top of each other in the z-direction.

2.1 Crystalline liquid crystals

For a perfect, infinite crystal, the intensity of R-π is infinitely sharp. We created a model with perfectly aligned columns. Each columns originates at z=0 and all other points in the column are equally spaced 3.7 Å apart in the z-direction (Figure 1). This essentially creates layers of atoms. The intensity of R-π for systems of various size are shown in Table 1. The intensity of R-π is equal to the number of atoms in the unit cell. The intensity will approach infinity as the system size becomes infinitely large.

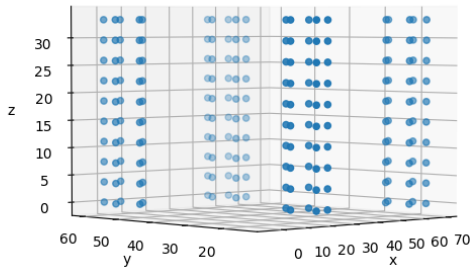

Figure 1

We measured the peak width of R-π in the q_r direction using the appropriate slice of the structure factor. Ideally, one should use the angle averaged structure factor for this calculation, but since the angle averaging procedure interpolates between bins, the averaged intensities are lower than expected which slightly changes the shape of the peak and gives misleading results. This reflection is radially symmetric about the z-axis, so we fit peak widths to cross-sections at $(0, y, 1.7)^{-1}$ Å(See Figure 2).

The distance, d, between peaks in the q_y cross-sections of the structure factor is equal to $2\pi/d$ (Figure 2). We looked at systems with pores spaced 42.5 nm and 212.5 nm apart respectively. The fundamental frequency appears at $q_y = 0$ with magnitude equal to the number of atoms in the unit cell (Note that each system has

L_z (Å)	Points per column	Number of Pores	Number of Atoms	R-π Intensity
14.8	4	4	80	80
18.5	5	4	100	100
37	10	4	200	200
14.8	4	9	180	180
18.5	5	9	225	225
37	10	9	450	450
14.8	4	16	320	320
18.5	5	16	400	400
37	10	16	800	800

Table 1: The intensity of R-π in a perfect crystal is equal to the number of scatterers in the unit cell. Here, L_z is the length of the unit cell in the z direction which corresponds to number of points per column $\times$ 3.7.

a different number of atoms). Subharmonics follow the fundamental frequency at equally spaced intervals of width $2\pi/d$.

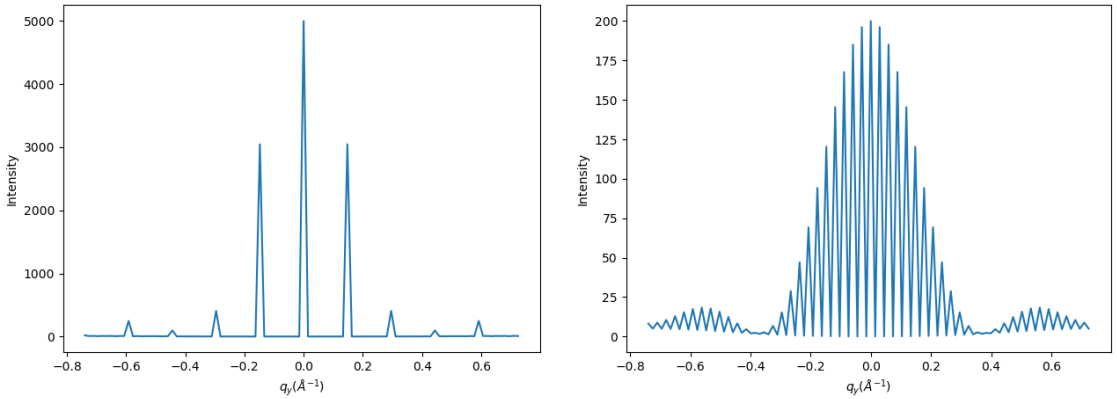

Figure 2: The distance between peaks of the structure factor cross-section at (0, y, 1.7) is equal to the distance between pores in q-space. The center peak of each distribution shows the fundamental frequency. The peaks that follow at higher $|\mathbf{q}|$ values are subharmonics. Both systems shown are in unit cells with dimensions of 42.5 x 42.5 x 3.7 nm. (a) We held the pore-to-pore spacing constant at 42.5 Å. The unit cell consists of 100 total pores. The first peak off-center peak is located at $q_y = .148\mathring{A}^{-1}$ which corresponds to $2\pi/.148 = 42.5\mathring{A}$ in real space. (b) We placed four pores in a unit cell spaced 212.5 Å apart. The first peak appears where expected at $q_y = 0.0296\mathring{A}^{-1}$ $(2\pi/212.5\mathring{A})$ and all other peaks are separated by that same distance.

We quantified the peak width by fitting gaussian curves to the R-π peak cross-sections and measuring ther full width at half maximum. Gaussian profiles appear to give the closest fit to the data (see Figure 3). We calculated all of FWHMs in Table 1 using gaussian fits.

IMPORTANT: Note that these 'peak widths' are not the same peak widths that are seen experimentally. If these showed up experimentally, they would appear as dots parallel to the q_r axis, crossing through R-π and in line with R-pores. There is some evidence of this occuring in some of the simulations (ordered parallel displaced for example).

The distance between pores does not affect the FWHM of the R-π 'peak' in the q_y direction. We held the size of the unit cell constant at 42.5 x 42.5 x 3.7 nm and varied the number of pores (and consequently, the distance between pores). We generated error bars for the fits based on the covariance of the optimized fit parameters. There is no statistical difference between the calculated values of each FWHM (Table 4). The uncertainty is lower for systems with less pores since there are more subharmonics available for curve fitting.

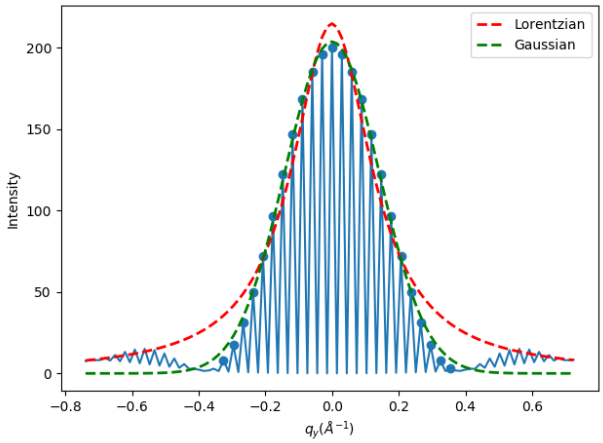

Figure 3: The gaussian functional form more closely matches the data than the Lorentzian functional form. Shown is data for a perfect crystal system with 4 pores and 4 points per column.

L_z (Å)	Number of Pores	Distance between Pores	R-π intensity	FWHM ($\AA^{-1}$)
37	4	212.5	200	0.372 ± 0.004
37	25	85.0	1250	0.371 ± 0.008
37	100	42.50	5000	0.375 ± 0.013

Table 2: We held the size of the unit cell constant at 42.5 x 42.5 x 3.7 nm and varied the number of pores and distance between pores. The value of FWHM is indistinguishable between the systems.

The finite FWHM of perfectly crystalline systems is due to non-uniform ordering of the columns within the pores. Although all scatterers are aligned and equally spaced in the z-direction, the individual columns of scatterers are offset from the pore center. Therefore, there is a range of similar but different distances between scatter scatterers. There are many opportunities for constructive and destructive interference with wavelengths slightly different than those which contribute to the fundamental frequency. If we place only one column at each pore center, the FWHM becomes infinite (See Figure 4)

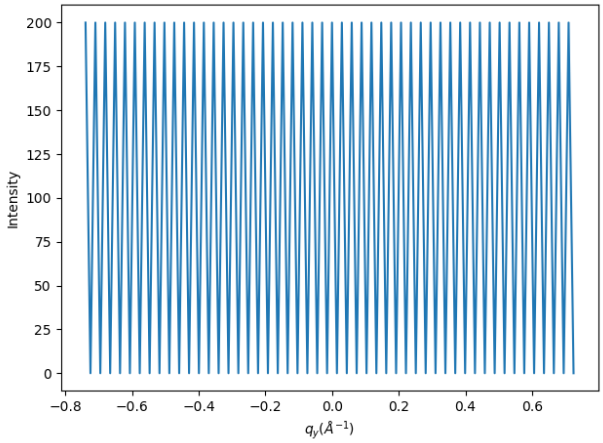

Figure 4: We placed one column of scatterers at each of 4 pore centers, spaced apart by 212.5 nm. Since the y-component of the distance between all scatterers is the same in all cases, subharmonics appear just as strongly as the fundamental frequency. Since the intensity doesn't decay, the FWHM is infinite.

The real system is far from a perfect crystal. Here we explore the influence of 4 sources of disorder on the intensity of R-π:

1. Random z-displacement of columns with respect to all other columns
2. Random rotation of layers about the z-axis
3. Thermal noise
4. Finite correlation between scatterers in the z-direction

2.2 Imperfectly aligned columns

We randomly aligned columns along the z-axis by adding a random displacement to each column of points. This simulates a system in which columns are uncorrelated. We shifted coordinates where necessary so that all atoms stayed within the unit cell. We held the spacing between each point within each column at 3.7 Å. We created trajectories of 1000 independent configurations in order to calculate the average intensity of R-π. 1000 independent configurations gives a reasonably converged average, enough to observe trends.

The intensity of R-π is equal to the number of scatterers per column when we randomly displace columns with respect to each other (See Table 4). It is independent of the number of pores (and hence number of columns) in the system. The error in the calculated intensities are comparable to the magnitude of the intensity because the intensity of each configuration in the trajectory fluctuates so much.

L_z (Å)	Points per column	Number of Pores	R-π Intensity
14.8	4	4	3.98
18.5	5	4	5.05
37	10	4	10.08
14.8	4	9	4.06
18.5	5	9	4.78
37	10	9	10.19
14.8	4	16	4.01
18.5	5	16	4.95
37	10	16	9.61

Table 3: The intensity of R-π is equal to the number of scatters in each column when columns are uncorrelated.

The q_y width of R-π is infinite when columns are randomly displaced in the z-direction. We attempted to measure the FWHM of the system with randomly displaced columns containing 4 pores and $L_z = 37$. The cross-section (Figure 5a) shows non-decaying noise centered near 10, the same R-π intensity in Table 4. The angle averaged pattern (Figure 5b) further illustrates the diffraction lines which characterize this type of system.

2.3 Randomly rotated layers

We observed the influence of correlation between layers by randomly rotating layers of scatterers about the z-axis. We held constant the angle, with respect to the pore center, between scatterers for any given layer. For example, since there are 5 columns per pore, each layer is made of 5 monomers. The angle made between the two vectors extending from the pore center to two adajacent scatterers in a single layer is 72 ° with respect to the xy plane.

In all cases, the maximum intensity of R-π is equal to the number of scatterers in the system and the FWHM of the q_y cross-section of the structure factor at R-π is 0.37 $\mathring{A}^{-1}$, just as the perfect crystal.

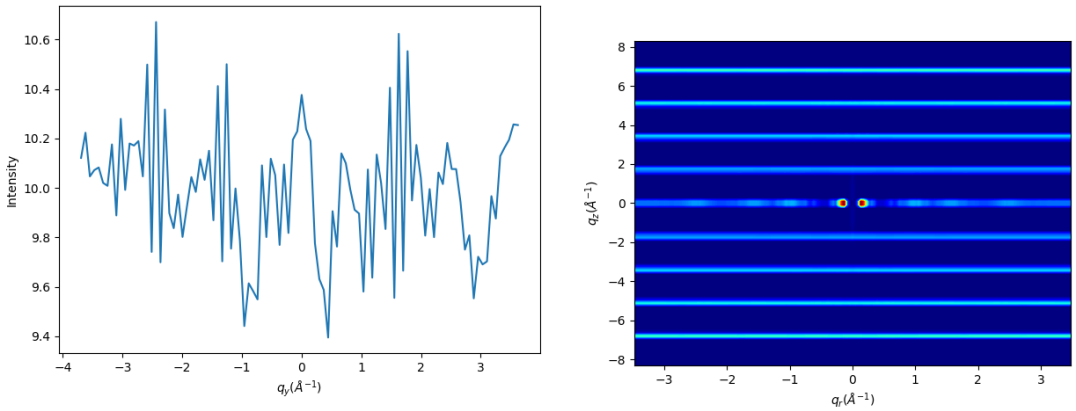

(a) (b)

Figure 5

L_z (Å)	Points per column	Number of Pores	Number of Atoms	R-π Intensity	FWHM $\AA^{-1}$
14.8	4	4	80	80	0.37
18.5	5	4	100	100	0.37
37	10	4	200	200	0.37
14.8	4	9	180	180	0.37
18.5	5	9	225	225	0.37
37	10	9	450	450	0.37
14.8	4	16	320	320	0.37
18.5	5	16	400	400	0.37
37	10	16	800	800	0.37

Table 4: The intensity of R-π is equal to the number of scatters in each column when columns are uncorrelated. Note that reproducing these results requires a very fine histogram, and thus a much more expensive calculation. The default binning scheme (100 bins in each dimension) gives slightly misleading answers.

2.4 The influence of thermal disorder

We added gaussian noise in each dimension to observe its influence on the intensity of R-π and the FWHM. For the z-direction, the standard deviation of the gaussian distribution is equal to a fraction of the average distance between scatterers in columns (d). In the xy-directions, the standard deviation is equal to a fraction of the pore radius (r).

2.4.1 Randomly displaced columns

When we add noise in the z direction, the intensity of R-π decays while the FWHM remains infinite (Figure 6a).

When we add noise in the x and y directions, R-π has a finite peak width in its q_y dimension (Figure 6b), and the intensity stays constant. We fit a Gaussian function to the the q_y cross-section in order to determine its FWHM. The FWHM decay is inversely proportional to the amount of noise added (Figure 6c).

This mode of broadening of R-π is more consistent with the experimental pattern, where the q_y cross-section of R-π is a continuous, broad peak.

2.4.2 Randomly rotated layers

When we add noise in the z direction, the intensity of R-π decays to 1 rapidly (Figure 7a), much like the decay shown in Figure 6a. The FWHM slowly increases until it jumps to infinity when the intensity of R-π

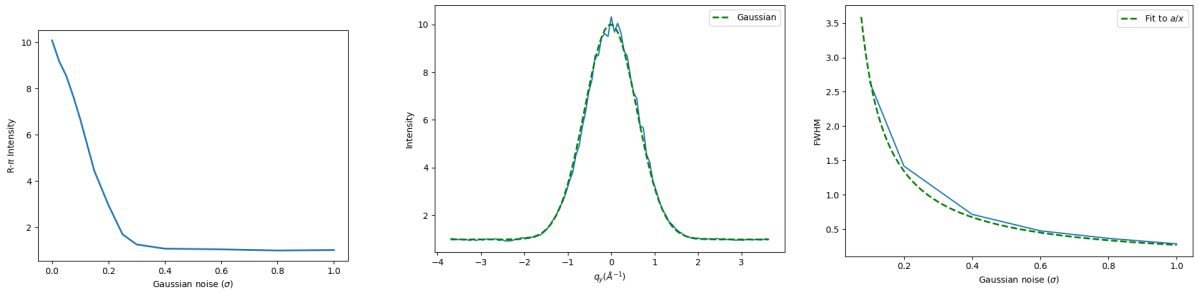

(a) (b) (c)

Figure 6: (a) The intensity of R-π decays to 1 rapidly as gaussian noise is added to the system. (b) When we add noise in the x and y directions, R-π broaden in the y-direction with a continuous intensity distribution that can be fit to a gaussian. (c) This FWHM decreases as the inverse of the amount of noise added.

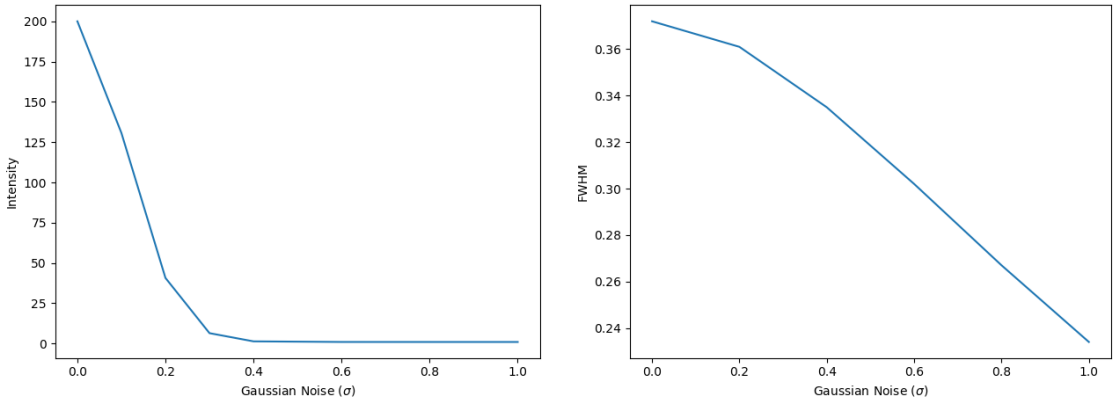

(a) (b)

Figure 7: (a) As we add noise in the z-direction, the intensity of R-π decreases rapidly to 1. The FWHM decays slowly and then jumps goes to infinity (not pictured) when the intensity of R-π becomes equal to the background intensity. However one could argue there is no peak at that point. (b) When we add noise in the x and y directions, the intensity of R-π does not change, but the FWHM decays slowly.

is comparable to the background intensity.

When we add noise in the x and y directions, the intensity of R-π does not change. The FWHM slowly decays as shown in Figure 7b. Importantly, the peak is defined by spikes like those shown in Figure 2.

2.5 Finite z-correlations

The z-cross-section of the R-π peaks are delta functions in all of the above systems (See Figure 8). None of the routes explored so far show how R-π might broaden in the q_z direction. The delta-function behavior does not change when the system is made taller so as to increase the resolution in z. We built a system 10x taller (37 nm), added random column displacement and some noise in the z-direction. R-π is still a sharp delta function (Figure 9).

(Please let me know if there is a more correct way of doing this) We added a correlation length to scatterers in z-direction. To do so, we define a covariance matrix to describe the correlation between all pairs of scatterers. The variance is defined so that the covariance in position of a scatterer with itself is the same for all scatterers. The covariance in position between scatterers decays exponentially from v according to the equation $ve^{-z/L}$ where L is the correlation length. Note that in its current implementation, it does not take periodicity into account, so a correlation length shorter than the box is necessary. A visualization

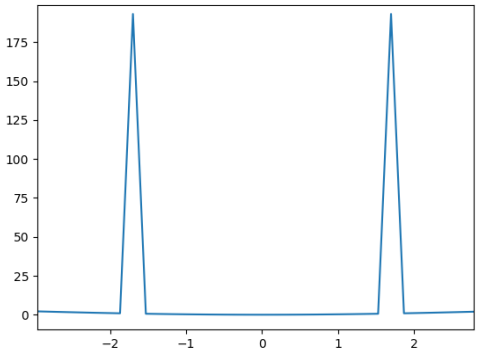

(a) Perfect Crystal

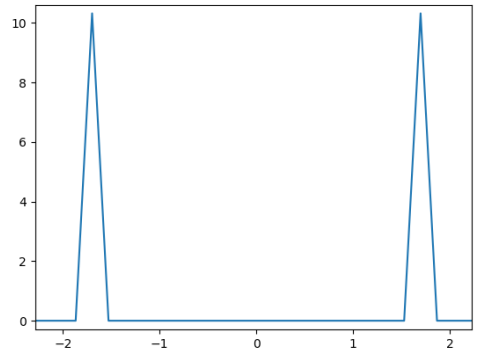

(b) Randomly displaced columns

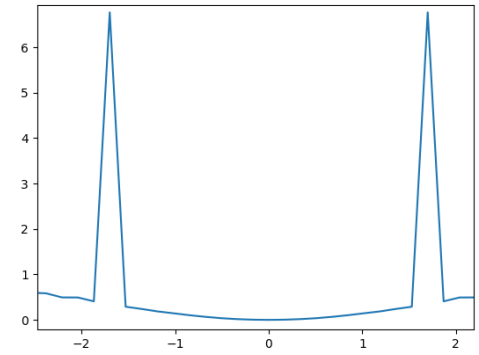

(c) Randomly displaced columns w/ z-noise

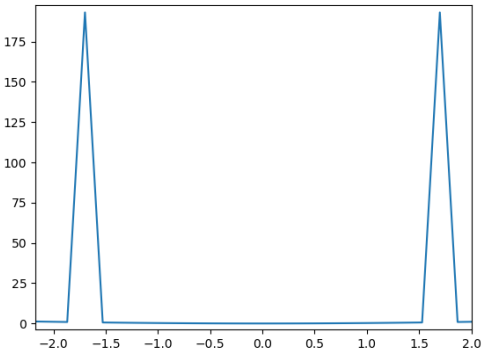

(d) Randomly rotated layers w/ xy-noise

Figure 8: Several examples of the delta-like behavior of R-π. Randomly displacing columns, randomly rotating layers, and adding thermal disorder do not broaden the z-cross-section of R-π.

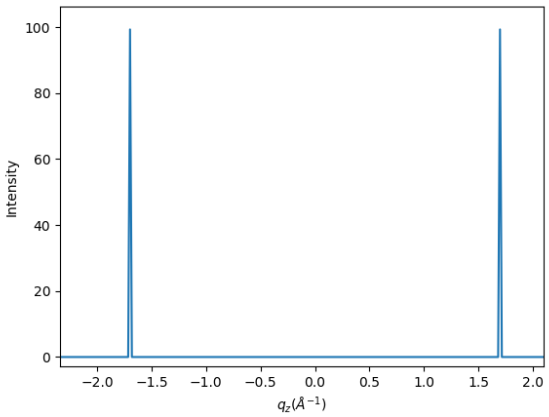

Figure 9: R-π still appears to be a delta function even with higher resolution and noise in the z-positions of the scatterers

of a typical covariance matrix for a column containing 20 scatterers is shown in Figure 10. Next, we drew random samples from a multivariate normal distribution defined using the covariance matrix, and applied these shifts to the columns of scatterers.

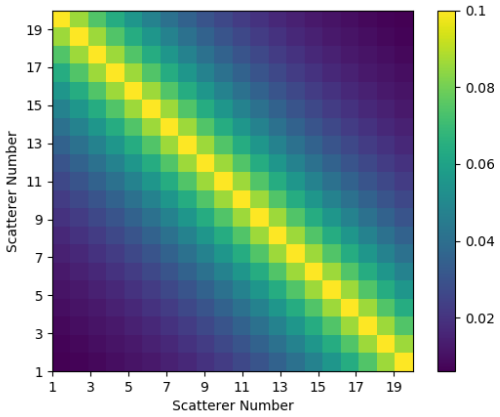

Figure 10

Adding a finite correlation length between scatterers causes R-π to broaden in the q_z direction. We simulated a system with dimensions of 8.5 x 8.5 x 37 nm, so that there would be 100 scatterers in the z-direction and a fourier bin size of $1/370 = 0.0027\AA^{-1}$. There is a clear broadening of R-π when scatterers are correlated (Figure 11a). The maximum intensity of R-π decreases as the variance in scatterer position increases (Figure 11b), however the intensity of R-π does not change when we vary the correlation length while holding the variance constant.

3 Conclusion

A number of factors influence the shape and intensity of the R-π reflection. The maximum intensity of the reflection is most strongly influence by thermal disorder in the z-direction. The peak is broadened in the q_y (q_r) direction when there is xy-direction thermal disorder in systems with randomly displaced columns. The peak is broadened in the q_z direction when there is a finite (non-zero) correlation length between scatterers.

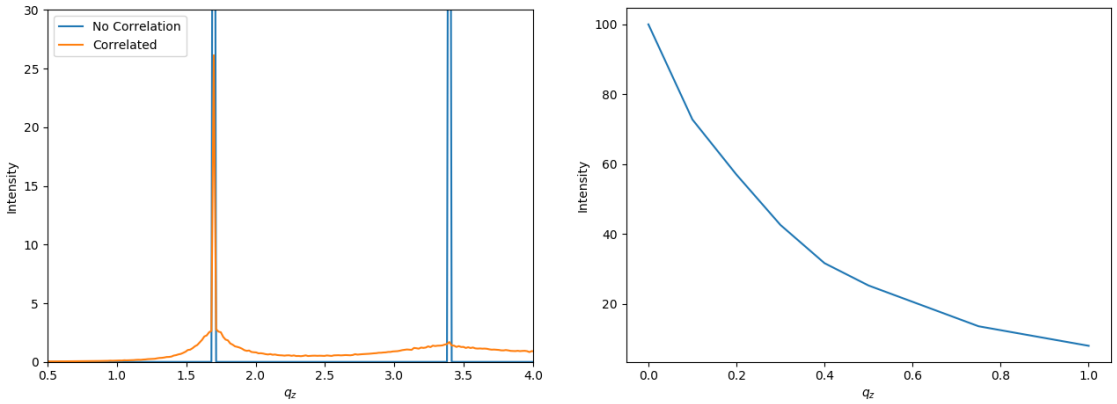

(a) (b)

Figure 11: (a) R-π broadens in the q_z direction when scatterers are correlated. (b) The intensity of R-π as the variance in scatterer position increases.